

# Online supplementary material for “Common Factor Cause-Specific Mortality Model”

## S.1 Model Estimation Procedure Overview

Here we will provide a summary of the steps taken in the research. For a more detailed description we used reference numbers to the sections in this paper. Note that all steps (except the reestimation step) are done for both male and female separately.

1. **Crude mortality:** For cause  $c$  and population  $i$ , we obtain the crude cause-of-death mortality  $m_i^c(x, t)$  for age  $x$  in year  $t$  using Equation (2).
2. **Marginal survival:** We obtain the marginal cause-specific survival function  $S_i^c(x, t)$  through Equation (13). Henceforth, all steps are performed for both Frank as well as Clayton copula specification.
3. **Net mortality:** The net mortality intensities  $\lambda_i^c(x, t)$  can be derived directly from each net survival function. Equation (16) provides the corresponding method.
4. **Common factor estimation:** We derive the common factor parameter estimations by performing step 1 from Section 2.3 for the obtained marginal mortality values of EU.
5. **Population effect estimation:** Using the results of the previous step and the marginal mortality from NL data, we estimate the parameters explaining the individual population mortality effects by means of step 2 (Section 2.3).
6. **Reestimation:** By means of the steps described in Section 2.4, we reestimate the time dependent set of variables for male and female simultaneously.
7. **Forecast:** We forecast the net mortality 45 years using the time series analysis from the previous step.
8. **Inverse transformation:** We implement Equation (16) reversely and afterwards apply Equation (14) to acquire crude mortality forecasts. For this we use forecast general mortality (see Equation (3)) using the LL model.
9. **Logistic extrapolation:** Extrapolate the crude mortality forecasts using the theory of Kannisto (1994) for old age mortality.

The resulting set of information are crude mortality forecasts from 2016 to 2060, for ages 0 to 120 and all causes of death included in the data. The results are for male and female separately and we differentiate between results under the assumption of either a Frank or Clayton survivor copula.

## S.2 Data manipulation

Table S1 presents the last year before the next classification method was adopted for each country within the time period 1970-2015. In line with leading literature, we have bundled data of deaths due to similar causes instead of analysing certain diseases separately. We consider five major categories of diseases for our research: Circulatory system, Cancer, Respiratory system, External causes and Infectious/parasitic diseases. These are the same groups as used by Arnold and Sherris (2015) and (excluding infectious/parasitic diseases) Li and Lu (2019). These groups constitute more than 80%

of the deaths in the past years and around 60% to 70% half a decade ago (Arnold and Sherris 2013). Moreover, we have included total deaths of each country to the data set, for reasons explained later in this section. The corresponding coding for the various causes, as found in the WHO mortality database handbook, is shown schematically in Table S2.

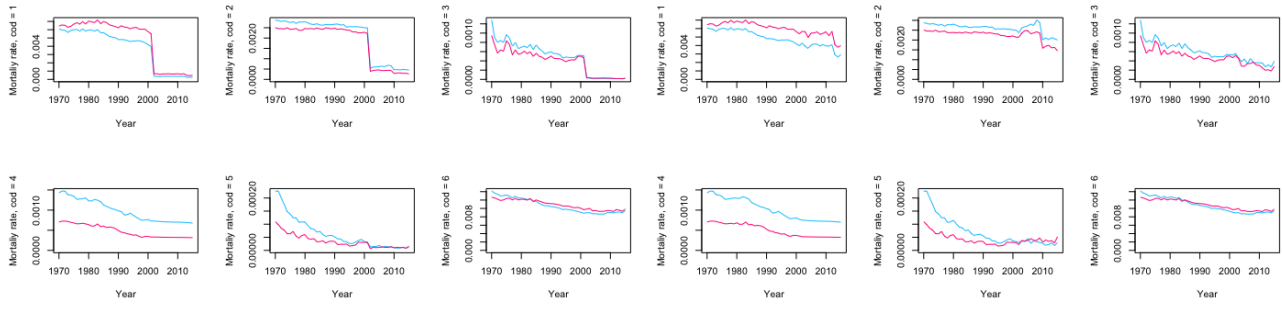
Table S1: Final year of implementation of the ICD codes per country for the total cause-specific data set 1970-2015.

Country	ICD-7	ICD-8	ICD-9	ICD-10
Austria	-	1979	2001	2015
Belgium	-	1978	1997	2015
Denmark	-	1993	-	2015
Finland	-	1986	1995	2015
France	-	1978	1999	2015
Germany	-	-	1990-1997	2015
GDR	-	1978	1989	-
FRG	-	1978	1989	-
Iceland	1970	1980	1995	2015
Ireland	-	1978	2006	2015
Luxembourg	1970	1978	1997	2015
Netherlands	-	1978	1995	2015
Norway	-	1985	1995	2015
Sweden	-	1986	1996	2015
Switzerland	-	1994	-	2015
United Kingdom	-	1978	1999	2015

Table S2: Cause-of-death coding of the different classification systems.

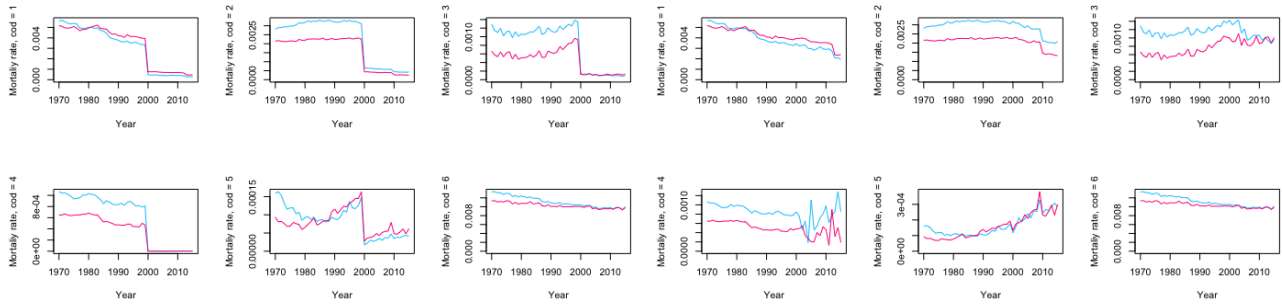
Code	Causes of death	ICD-7	ICD-8	ICD-9	ICD-10
1	Circulatory system	A079-A086	A080-A088	B25-B30	I00-I99
2	Cancer	A044-A060	A045-A061	B08-B17	C00-D48
3	Respiratory system	A087-A097	A089-A096	B31-B32	J00-J99
4	External causes	A138-A150	A138-A150	B47-B56	V00-Y89
5	Infectious and parasitic diseases	A001-A043	A080-A088	B01-B07	A00-B99
	Total	A000	A000	B00	AAA

After having applied the filters described in the previous part, we end up with a data set including 14 countries and 5 cause-of-death categories. This comprehensive data set does involve a considerable amount of shortcomings and faults which need to be taken into account before continuing the research. In this section we expand on the action we undertook in order to amend these irregularities and data constraints. We discuss the subsequent data manipulation in the following sections: Comparability and Incomplete and Insufficient data.



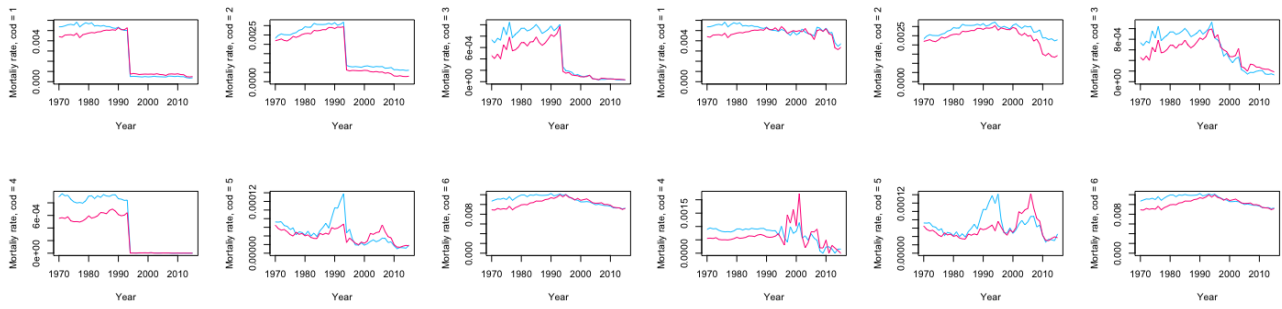
(a) Before (Austria)

(b) After (Austria)



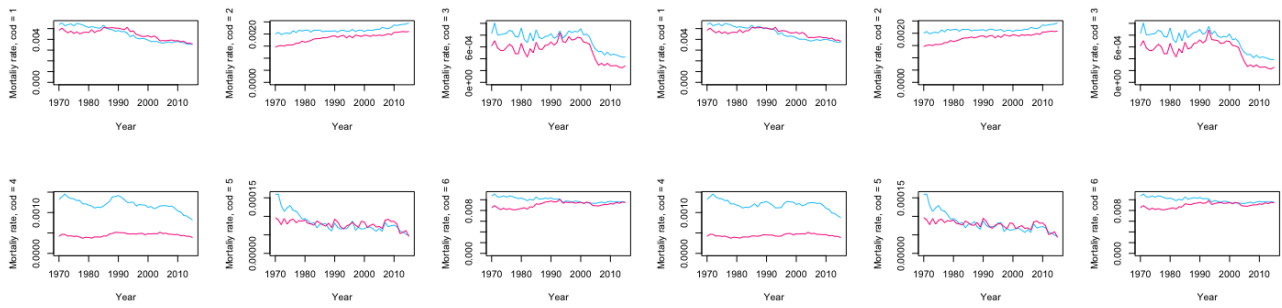
(c) Before (Belgium)

(d) After (Belgium)



(e) Before (Denmark)

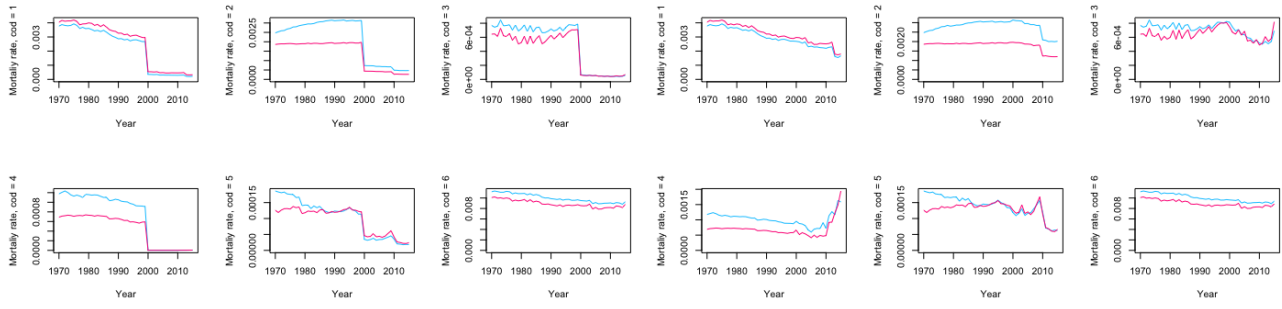
(f) After (Denmark)



(g) Before (Finland)

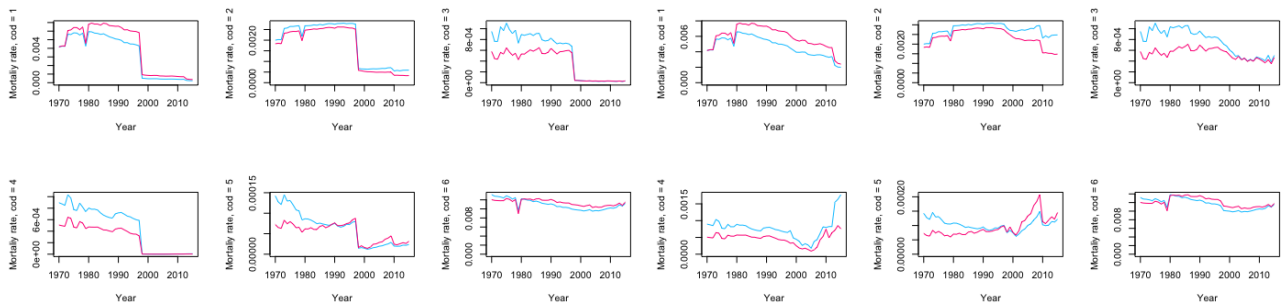
(h) After (Finland)

Figure S1: The effect of the comparability transformation.



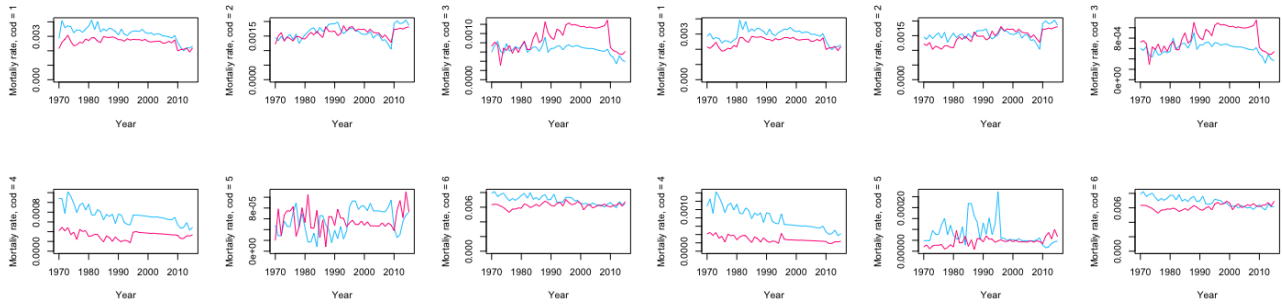
(a) Before (France)

(b) After (France)



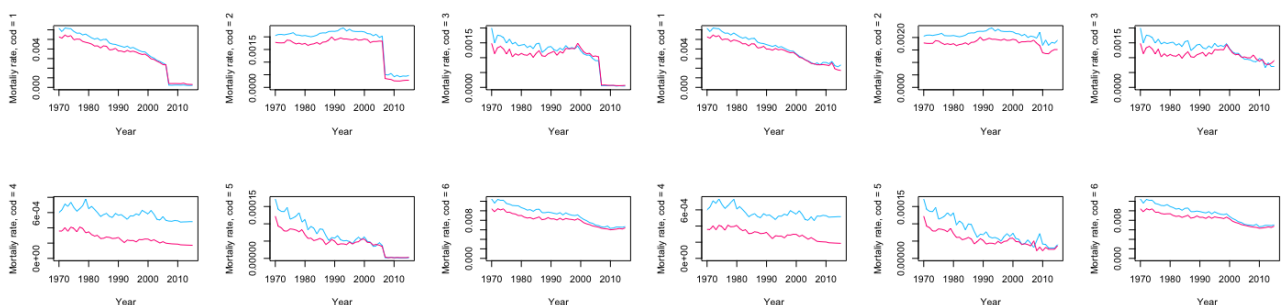
(c) Before (Germany)

(d) After (Germany)



(e) Before (Iceland)

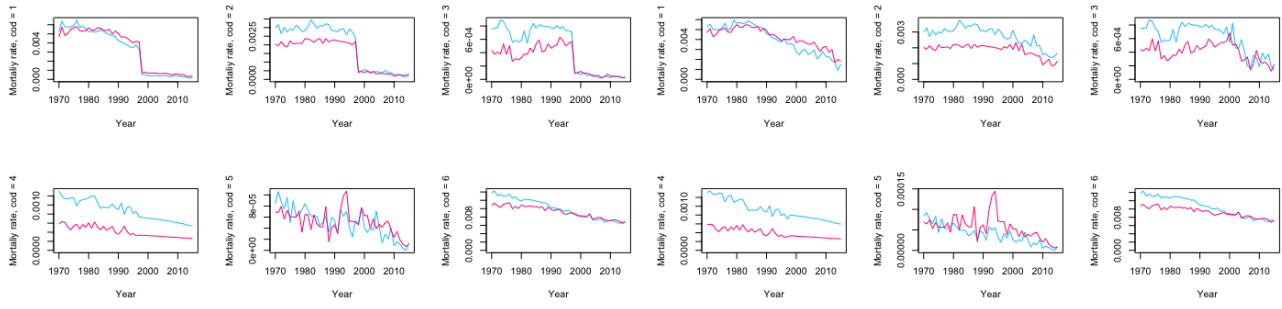
(f) After (Iceland)



(g) Before (Ireland)

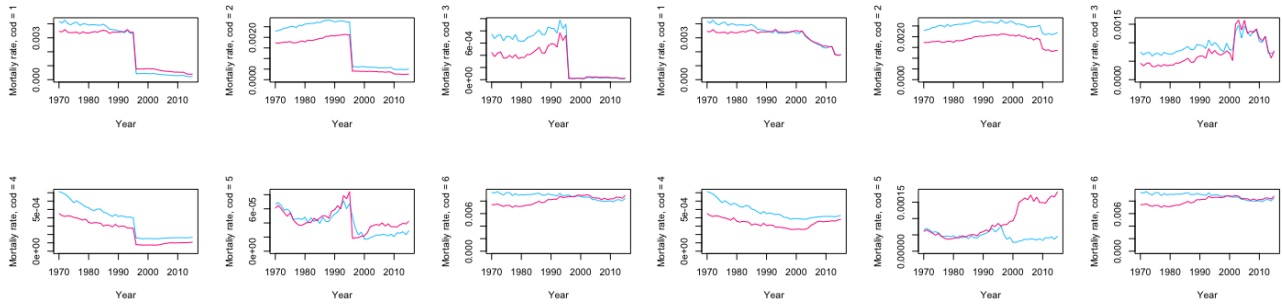
(h) After (Ireland)

Figure S2: The effect of the comparability transformation.



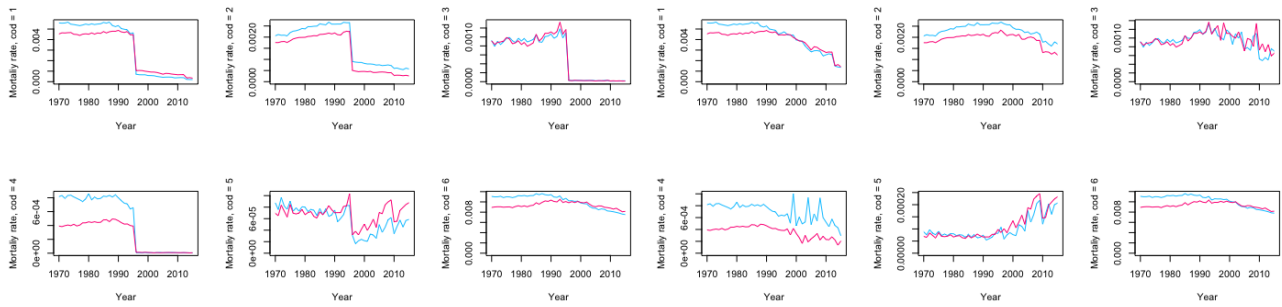
(a) Before (Luxembourg)

(b) After (Luxembourg)



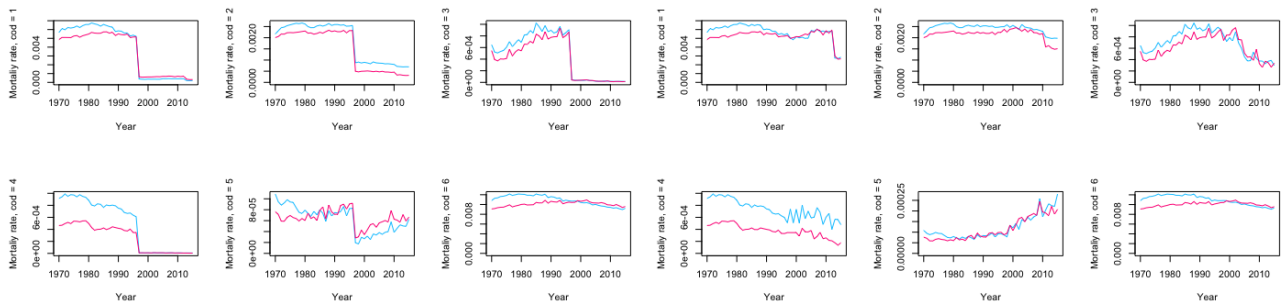
(c) Before (Netherlands)

(d) After (Netherlands)



(e) Before (Norway)

(f) After (Norway)



(g) Before (Sweden)

(h) After (Sweden)

Figure S3: The effect of the comparability transformation.

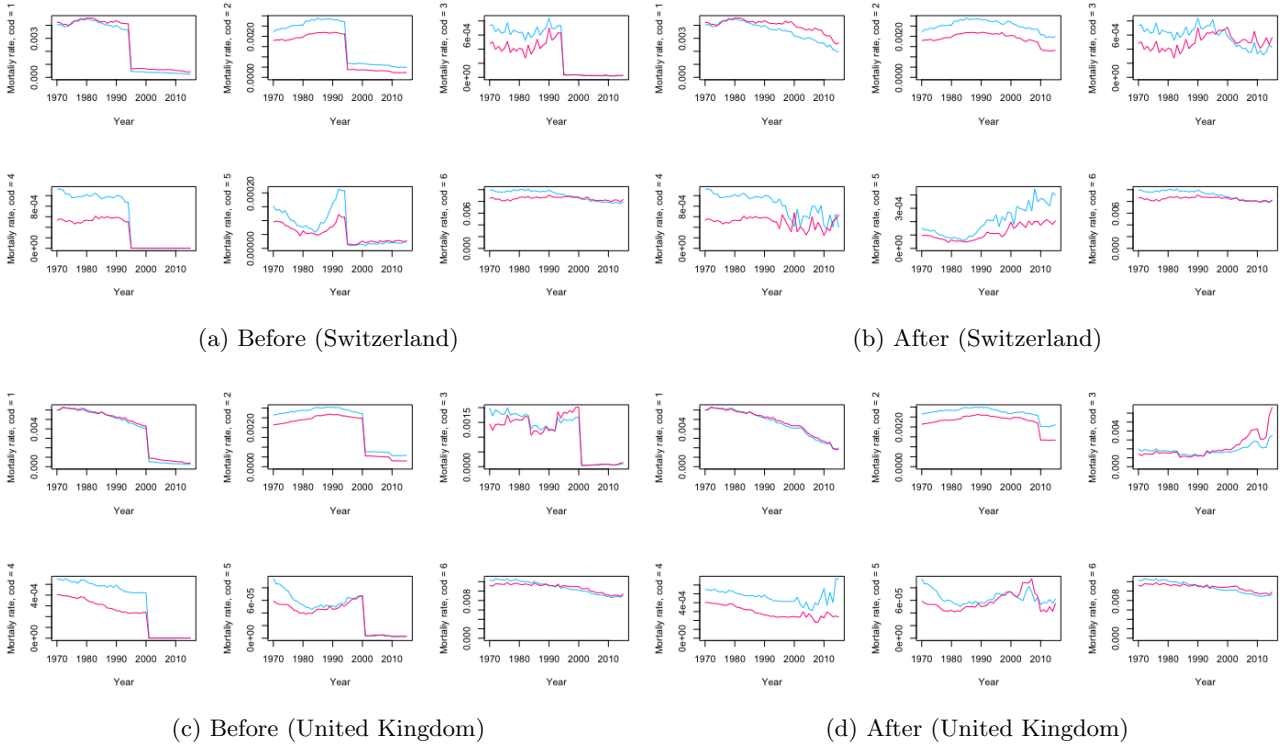


Figure S4: The effect of the comparability transformation.

### Comparability

In Table S1 we pinpointed the transition moments from one classification to another. As a consequence of adopting new methods of recording mortality data, the data of the successive classifications are analogous.

In Figures S1(a) to S4(d) we find that at the points of transition for some countries and some causes of death the data is not comparable, which appears as a steep drop or a steep rise at the according year. These disturbances are countered via the same method applied by Gaille and Sherris (2011), namely with the application of comparability ratios. The comparability ratio is acquired by the condition that the average cause-of-death specific mortality in the last two years before the transition should equal the mean cause-of-death specific mortality of the two years following the transition. Suppose the first after the transition is  $t = A$  and the last year before the transition is  $t = B$ , then mathematically:

$$\frac{\mu_B + \mu_{B-1}}{2} = c \cdot \frac{\mu_A + \mu_{A+1}}{2}, \quad (\text{S1})$$

where  $c$  denotes the comparability ratio. After having calculated the comparability ratio, we multiply cause-of-death specific mortality for all years that fall under the new system. We apply this for every country and every cause of death to maintain continuity over different classifications. The results are found in Figures S1(a) to S4(d).

The simplicity of this method is advantageous, but the transformation described in Equation (S1) includes a considerable downside. Figures S1(a) to S4(d) show that in most cases, in particular for the transition to ICD-10, reported mortality lies significantly lower than is the case for the preceding phase. This, in turn, leads to a high corresponding comparability ratio. As a direct result, any deviation in the phase that is less rich in information is enhanced, increasing the volatility of mortality in this time period. Next section we discuss the cases in which this aspect becomes problematic and we

bring forward a solution.

### Incomplete and insufficient data

This section we will discuss the defects inherent with the raw data set as provide by WHO. For the countries GDR, Switzerland and United Kingdom the data for years 1979, 1994 and 2000 are missing, respectively. The missing data is most likely caused by the transition from one classification system to another which has occurred in all three specific cases. In order to cope with the absence of information for these specific countries in these specific years, we have assumed the number of deaths to be the same as the year before. The sometimes non-conform death levels between two classification periods, as discussed in the section on comparability, is the argumentation behind not choosing to use linear interpolation.

Furthermore, we previously observed that within our data set for some countries there exists a lack of sufficient information on some cause-of-death specific mortality within the last classification scheme, ICD-10. Generally, this issue is overcome with the use of the earlier discussed comparability ratio. Nevertheless, in some cases, there still exists too little data on mortality and in others no information at all. The former could result in a too large comparability ratio leading to an unrealistically high mortality volatility and the latter even leads to the absence of a comparability ratio. For the instances involving no information, we opted for either linear interpolation between the two enclosing years that contained sufficient information or linear extrapolation using the gradient as the preceding years. For the occurrences with too little information, we added the last year with sufficient information as a basis to the years with the shortage in data. In Table S3 we created an overview of these instances.

Table S3: Details of manipulated instances for insufficient data.

Country	Cause of death	Period	Method*
Austria	4	2002 - 2015	Basis
Iceland	4	1996 - 2009	Interpolation
Ireland	4	2007 - 2015	Extrapolation
Luxembourg	4	1998 - 2015	Basis

\*The three methods used to substitute the lack of data are: linear interpolation between surrounding years, linear extrapolation based on preceding years or add the level of deaths from the last year with sufficient information to the insufficient years.

After these alterations, we obtain a data set containing total mortality levels and mortality for 5 major groups of diseases and the mid-year population numbers for 14 different countries. The mortality intensities can be found in figure S5. In the graphs we indeed recognise the increased volatility for data from classification ICD-10. We accumulate these mortality numbers into one collection of cause specific mortality data and combined with the population figures will from now on be referred to as EU.

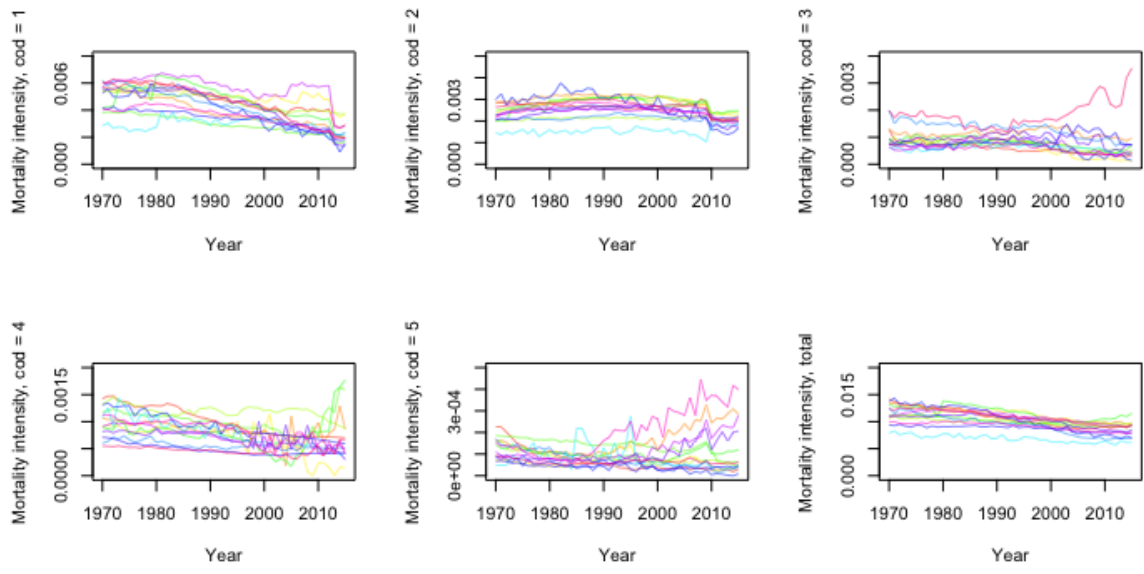


Figure S5: Cause-specific mortality intensities of the 14 selected countries in the data set after coping with the inherent data difficulties (1970–2015).

**Age groups**

The WHO data set provides an extensive amount of information on cause-of-death mortality. The number of deaths and population volumes per age are reported in varying ways. For certain years and certain countries the used age specific formatting distinguishes between the age-groups in a more detailed fashion than another country in the same year or the same country in a different year. For the whole WHO data file there are ten different age formatting methods used, however for the 14 selected European countries only three of these apply (see Table S4), namely format 00, format 01 and format 02.

Table S4: WHO Mortality Database formatting.

Format number		
00	01	02
0	0	0
1	1	1-4
2	2	-
3	3	-
4	4	-
5-9	5-9	5-9
10-14	10-14	10-14
...	...	...
80-84	80-84	80-84
85-89	85+	85+
90-94	-	-
95+	-	-

Format 02 has population and death levels divided in five-year age-groups with the exception of age

group 0–4, which is split up in the age 0 and the age-group 1–4. The last group, constituting the highest ages, contains ages 85 and above. This amounts to a total of 19 separate age groups for format 02. Format 01 offers more detailed information about the age group 1–4 by splitting this group into four groups with a one year interval. Lastly, format 00 is an expansion of format 01 due to the addition of age groups 85–89 and 90–94. The final group now becomes ages 95 and above, resulting in a total of 24 separate age groups.

Desirably, we would preserve as much information from the data set as possible, but due to the randomness of the formatting within countries and years and the ensuing complexity because of it we have opted for an overall format 02 by bundling age groups 1, 2, 3 and 4 for format 00 and format 01 data points and by bundling age groups 85–89, 90–94 and 95+ for format 00 data points.

For our research, we aim to use mortality on a age interval of one year. Since the data sets at hand, both NL and EU, contain less detailed information due to the 5-year age groups, we use interpolation in order to expand the number of data points. We interpolate following a similar method as the one provided by the HMD Method Protocol by Wilmoth et al. (2007). We take a lower boundary  $l = 0$  and an upper boundary  $u = 91$ . This means that we assume that all death in age group 85+ occur before age 91. Next, we create a variable representing the cumulative distribution of deaths per year up to age  $x$ :

$$C(x, t) = \sum_{k=0}^{x-1} D(k, t), \text{ where } x \in [l, u]. \quad (\text{S2})$$

We apply the cubic spline interpolation method as described by McNeil et al. (2011), which employs the ‘Hyman filter’ (Dougherty et al. 1989; Hyman 1983) to ensure monotonicity and therefore implicitly non-negative deaths. This yields a cumulative distribution of deaths on a one-year interval from age 0 to 91. We proceed by applying the following formula to obtain the number of deaths per age  $x$ :

$$\hat{D}(x, t) = \hat{C}(x + 1, t) - \hat{C}(x, t), \text{ where } x \in [l, u - 1]. \quad (\text{S3})$$

The resulting data set  $\hat{D}(x, t)$  ranges from ages 0 to 90 for the years 1970-2015.

### Data completion

In the last stage of the data manipulation we create the last cause-of-death indicator, namely that referring to all other deaths besides the 5 major disease groups. We denote the remaining causes as cause of death 6. The mortality data, from this time forward called Other, is calculated by subtracting all deaths due to the 5 previously described causes from the total number of deaths. The procedure does carry some minor issues with it. As a result of the data transformations explained in S.2 and the occasional shortage of information in the WHO Mortality Database, for some ages (all between ages 5 and 20 for which mortality levels are generally low) in some years, the sum of all causes of death exceeds the number of deaths under total. This obviously should not be the case as this would indicate a negative number of deaths under cause Other. Suppose in year  $t$  this is the case for age  $i$ . We construct the new assumed mortality as follows:

$$D_6(x, t) = \begin{cases} \frac{D_6(0, t)}{D_6(0, t-1)} \cdot D_6(x, t-1), & \text{if } D_{Total}(x, t) - (\sum_{c=1}^5 D_c(x, t)) \leq 0 \\ D_{Total}(x, t) - (\sum_{c=1}^5 D_c(x, t)), & \text{otherwise.} \end{cases} \quad (\text{S4})$$

## S.3 Parameter estimates

### S.3.1 Maximum likelihood estimates

Through the formulation of the LL model from Section 2.3 using maximum likelihood estimation method described in Section 2.3 we model the marginal mortality intensities. The resulting set of parameters is  $\hat{\theta}^{c,g} \in \{\hat{A}_{eu}^{c,g}(x), \hat{B}_{eu}^{c,g}(x), \hat{K}_{eu}^{c,g}(t), \hat{a}_{nl}^{c,g}(x), \hat{b}_{nl}^{c,g}(x), \hat{k}_{nl}^{c,g}(x)\}$ . The estimates are presented in figures S6 to S11. First we will discuss the differences in estimates between an assumed Clayton or Frank survivor copula. After that we will highlight some estimate properties that stand out.

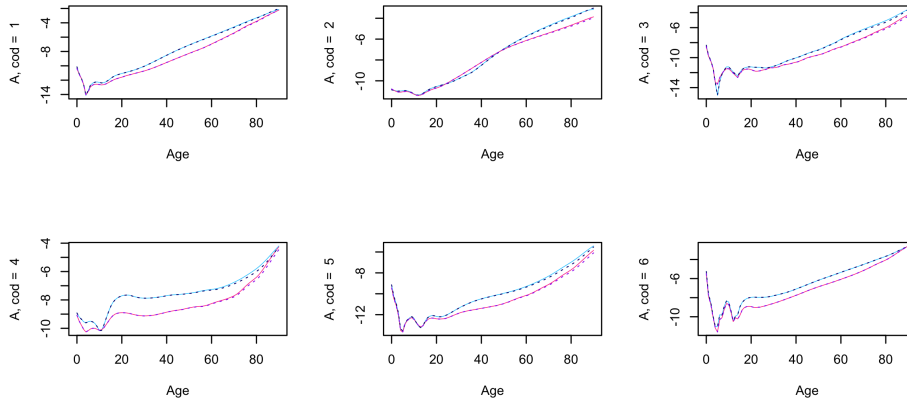


Figure S6: Age-specific constant for Frank (solid line) and Clayton (dotted line) models (EU).

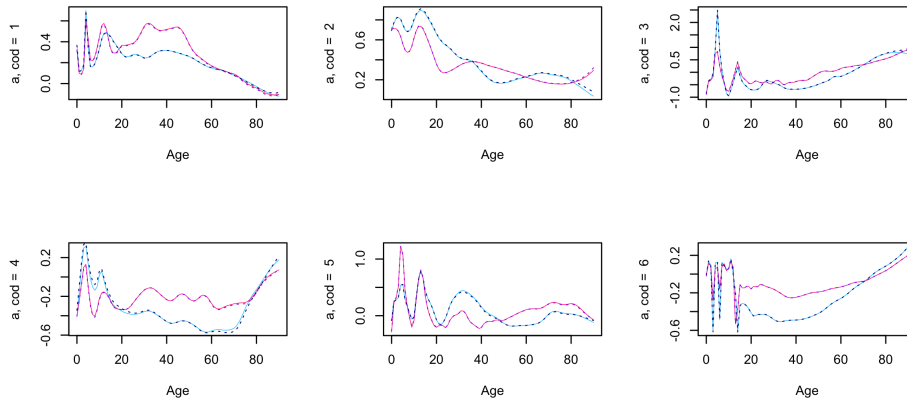


Figure S7: Age-specific constant for Frank (solid line) and Clayton (dotted line) models (NL).

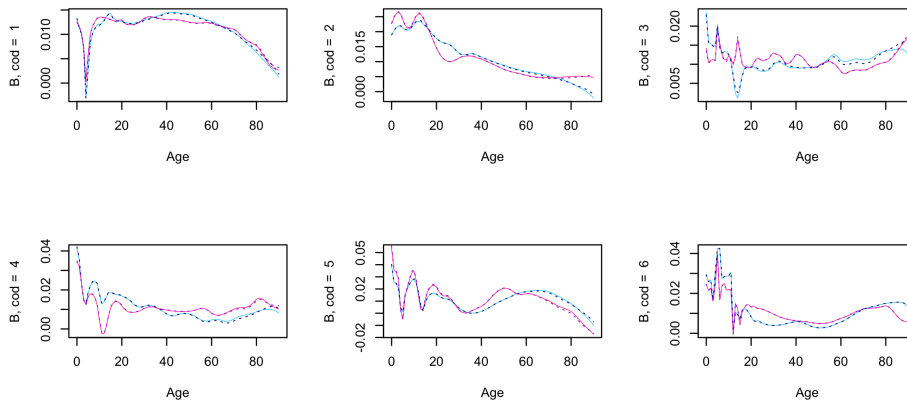


Figure S8: Age-specific trend sensitivity for Frank (solid line) and Clayton (dotted line) models (EU).

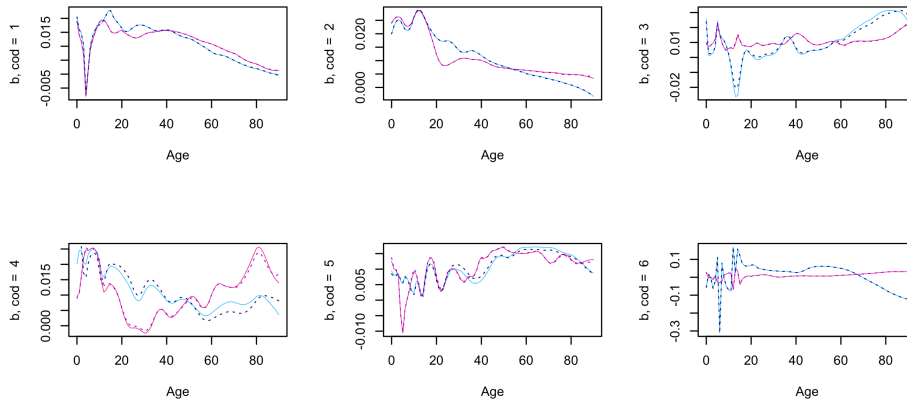


Figure S9: Age-specific trend sensitivity for Frank (solid line) and Clayton (dotted line) models (NL).

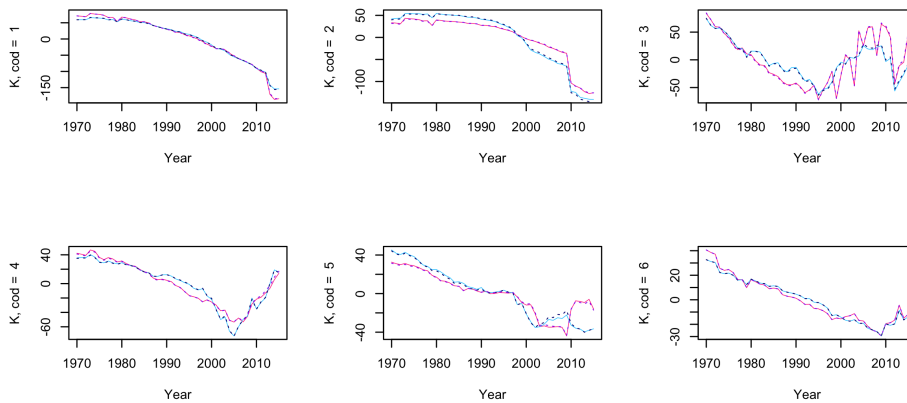


Figure S10: Time trend for Frank (solid line) and Clayton (dotted line) models (EU).

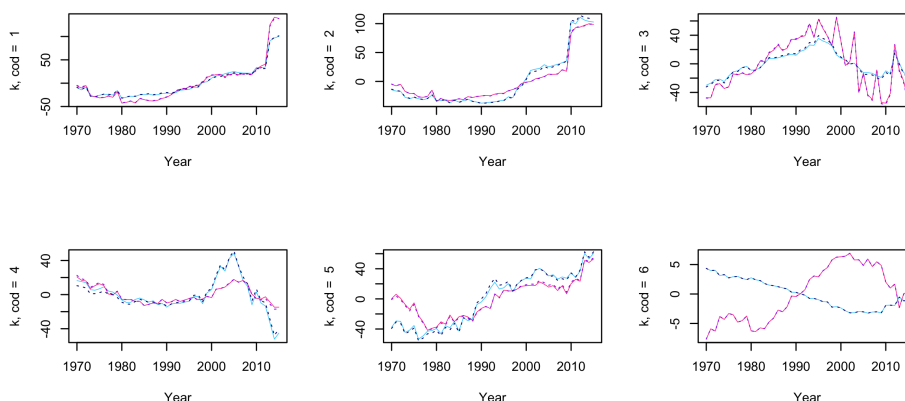


Figure S11: Time trend for Frank (solid line) and Clayton (dotted line) models (NL).

We start with the time dependent variable estimate for EU (figure S10). The trend of the time dependent coefficients is downwards for all causes of death. This implies, for positive age specific  $\hat{B}_{eu}^{c,g}(x)$ , a decrease of net mortality over time for all causes. The estimates are similar for both copulas. Only some minor differences can be determined. The time dependent variables for NL under Clayton and Frank assumption are comparable as well. We also determine from the results that for EU data, mortality trend has been upwards for respiratory diseases, external and other causes of death an infectious diseases (cod 3, cod 4, cod 5 and cod 6) in recent years. This is in contrast with past observed trends, which overall showed mortality to be decreasing. Dutch mortality trend with respect to EU shows fluctuating directions. For circulatory diseases, cancer and infectious/parasitic diseases (cod 1, cod 2 and cod 5) we see an general rising trend. Cod 3 (respiratory diseases) mortality trends goes up, only to fall back down again after 1995 and cod 4 (external causes) mortality shows a decreasing trend. Mortality from other causes (cod 6) shows opposite trends for males and females. This is in line with literature, which shows male and female mortality to converge (Antonio et al. 2017). For some causes we see bigger magnitude of changes after 2000. This complies with the data particularity of increased mortality volatility for ICD-10 for the EU data set from WHO. We determined a drastic reduction of information after the implementation of ICD-10, which for most EU countries occurred around the start of the millennium. In order to counter this we used the comparability ratios, which in turn increased data volatility. We observe that the time trend of NL compensates for this volatility, which can be clearly be observed for respiratory diseases (cod 3) for instance. In years where EU mortality jumps upwards, we see shocks downwards for NL mortality and vice versa. This implicates that NL data does not contain this erratic behaviour after the incorporation of ICD-10. This is a result of the alternative source that we have used for NL, namely CBS instead of WHO.

Next, we assess the age specific constant for EU, namely  $\hat{A}_{eu}^{c,g}(x)$ . No big difference between the Frank and Clayton estimates can be concluded. For all causes we see a high value for the early ages and a low point between age 5 and 10. Afterwards, the mortality constants rise steadily upward for both male and female. Lastly, we clearly see the bulge of mortality around the age of 20 for males (and females in a smaller degree) which corresponds with the observations from Section 4.1.

The estimated constant for NL data can be interpreted as an addition to the EU constant. If the value is positive it means that the time-invariant net mortality for Dutch population is higher than its EU complement. This is the case for circulatory diseases (ages before 80) and cancer (all ages).

The opposite is true for external causes (few ages excepted) and other causes (between ages 10 to 70). The remaining causes show results fluctuating from negative to positive and back. It follows from the results that the effects are more erratic for the younger ages as these age groups suffer from scarcity in observations.

Some minor differences can be noted for EU between the Clayton and Frank age-specific time sensitivity  $\hat{B}_{eu}^{c,g}(x)$ . These differences occur exclusively at older ages. All estimated values are positive, bar a few exceptions. For example, we see negative values for cod 5 (infectious and parasitic diseases) for the ages above 80 and 85 for females and males respectively.

Lastly, for the estimates of the age-specific time sensitivity of NL we see big differences for respiratory diseases, external causes and parasitic/infectious diseases (cod 3, cod 4 and cod 5) male mortality between the Clayton and Frank copula. This anomaly is also commented on in the paper by Li and Lu (2019) for respiratory diseases and external causes. They remark that two possible explanations can be pointed out. On one hand, it can question whether a strong dependence structure for these two causes is appropriate. The authors mention that a big portion of respiratory disease deaths result from bacterial infections. Therefore, respiratory diseases and likewise infectious and parasitic diseases can be strongly linked to personal health whereas external causes can not. Subsequently, twisted mortality trends can result. Moreover, since cod 4 and cod 5 comprise the smallest portions of total mortality, this distortion weighs stronger for these two causes of death.

An apparent upside of our common factor model formulation with respect to a single population cause-specific mortality model such as the one used in Li and Lu (2019), is the reduced sensitivity to incidental deviation of NL data. We first perform the parameter estimation for EU and sequentially estimate the model capturing the deviation of NL cause-specific mortality from that of EU. From the illustrations we can clearly see that in some cases this deviation is significant. Therefore, because we include EU data we estimate for much more data points which makes the estimation more reliable.

### S.3.2 Forecast parameter estimates

This section introduces the results from fitting an ARIMA(0,1,0) and ARIMA(1,0,0) model to the estimates  $\hat{K}_{eu}^{c,g}(t)$  and  $\hat{k}_{eu}^{c,g}(t)$ , respectively. The reestimation method is discussed in more detail in Section 2.4. The parameter values are given in Table S5.

Table S5: Estimated coefficients of the SUR reestimation of the estimated time dependent variables  $K^c = \{\hat{K}_{eu}^{c,M}(t), \hat{k}_{nl}^{c,M}(t), \hat{K}_{eu}^{c,F}(t), \hat{k}_{nl}^{c,F}(t)\}$ .

Copula	COD	$\hat{\rho}^M$	$\hat{\omega}^M$	$\hat{\rho}^F$	$\hat{\omega}^F$
Frank	1	-3.467	0.990	-3.295	0.971
	2	-1.309	0.991	-2.034	0.977
	3	-0.960	0.966	-1.238	0.963
	4	-1.357	0.905	-1.719	0.961
	5	-0.941	0.993	-1.560	0.979
	6	-0.529	0.942	-0.341	0.953
Clayton	1	-3.489	0.991	-3.305	0.973
	2	-1.236	0.991	-1.962	0.978
	3	-0.953	0.964	-1.232	0.963
	4	-1.268	0.909	-1.531	0.963
	5	-1.024	0.998	-1.507	0.979
	6	-0.529	0.943	-0.341	0.953

Below we present the covariance matrices of the reestimation of  $K^c = \{\hat{K}_{eu}^{c,M}(t), \hat{k}_{nl}^{c,M}(t), \hat{K}_{eu}^{c,F}(t), \hat{k}_{nl}^{c,F}(t)\}$  for both an assumed Frank survivor copula (S5) and an assumed Clayton survivor copula (S6).

$$\begin{aligned}
 H^1 &= \begin{pmatrix} 109.52 & -145.89 & 69.17 & -97.86 \\ -145.89 & 209.35 & -90.66 & 140.52 \\ 69.17 & -90.66 & 46.70 & -63.48 \\ -97.86 & 140.52 & -63.48 & 103.90 \end{pmatrix}, & H^2 &= \begin{pmatrix} 112.82 & -114.23 & 94.87 & -114.00 \\ -114.23 & 122.75 & -95.26 & 115.80 \\ 94.87 & -95.26 & 88.74 & -106.67 \\ -114.00 & 115.80 & -106.67 & 135.88 \end{pmatrix}, \\
 H^3 &= \begin{pmatrix} 881.13 & -704.60 & 155.00 & -87.90 \\ -704.60 & 616.35 & -100.30 & 80.60 \\ 155.00 & -100.30 & 187.82 & -82.81 \\ -87.90 & 80.60 & -82.82 & 47.08 \end{pmatrix}, & H^4 &= \begin{pmatrix} 33.67 & -15.16 & 33.88 & -27.04 \\ -15.16 & 17.74 & -19.78 & 20.08 \\ 33.88 & -19.78 & 72.91 & -70.60 \\ -27.04 & 20.08 & -70.60 & 74.93 \end{pmatrix}, \\
 H^5 &= \begin{pmatrix} 31.59 & 8.01 & -5.42 & -6.53 \\ 8.01 & 67.05 & -3.87 & 34.48 \\ -5.42 & -3.87 & 13.01 & -9.36 \\ -6.53 & 34.48 & -9.36 & 77.74 \end{pmatrix}, & H^6 &= \begin{pmatrix} 17.44 & -3.30 & 13.74 & 1.12 \\ -3.30 & 1.50 & -2.97 & -0.42 \\ 13.74 & -2.97 & 11.79 & 1.10 \\ 1.12 & -0.42 & 1.10 & 0.17 \end{pmatrix}.
 \end{aligned} \tag{S5}$$

$$\begin{aligned}
H^1 &= \begin{pmatrix} 110.94 & -149.95 & 73.64 & -103.42 \\ -149.95 & 218.51 & -97.97 & 150.24 \\ 73.64 & -97.97 & 51.49 & -69.56 \\ -103.42 & 150.24 & -69.58 & 111.83 \end{pmatrix}, & H^2 &= \begin{pmatrix} 117.83 & -118.00 & 105.41 & -122.25 \\ -118.00 & 125.57 & -104.78 & 122.69 \\ 105.41 & -104.78 & 102.20 & -118.71 \\ -122.25 & 122.69 & -118.71 & 145.62 \end{pmatrix}, \\
H^3 &= \begin{pmatrix} 903.60 & -728.79 & 156.08 & -97.21 \\ -728.79 & 645.22 & -100.42 & 90.62 \\ 156.08 & -100.42 & 190.39 & -90.06 \\ -97.21 & 90.62 & -90.06 & 55.76 \end{pmatrix}, & H^4 &= \begin{pmatrix} 33.04 & -15.15 & 33.17 & -26.56 \\ -15.15 & 17.99 & -20.62 & 20.57 \\ 33.17 & -20.62 & 71.39 & -69.01 \\ -26.56 & 20.57 & -69.01 & 71.98 \end{pmatrix}, \\
H^5 &= \begin{pmatrix} 30.42 & 7.69 & -8.80 & -3.71 \\ 7.69 & 66.43 & -5.06 & 36.43 \\ -8.80 & -5.06 & 15.93 & -10.42 \\ -3.71 & 36.43 & -10.42 & 81.44 \end{pmatrix}, & H^6 &= \begin{pmatrix} 17.44 & -3.304 & 13.74 & 1.12 \\ -3.30 & 1.50 & -2.97 & -0.42 \\ 13.74 & -2.97 & 11.79 & 1.10 \\ 1.12 & -0.42 & 1.10 & 0.17 \end{pmatrix}.
\end{aligned} \tag{S6}$$

We see that all drift coefficients (i.e.  $\hat{\rho}^M$  and  $\hat{\rho}^F$ ) are negative, which indicate a negative time dependence for all causes of death. This trend is best observed for cod 1, both male and female. Respectively, the corresponding drift coefficients respectively for male and female are  $-3.467$  and  $-3.295$  (Frank) and  $-3.489$  and  $-3.305$  (Clayton). The next biggest decreasing trends are for cod 2 and cod 4. The lowest decrease is observed for cod 6. In addition, we determine that for the Clayton copula the trend is similar to that of the Frank model.

When we turn to the autoregressive elements we conclude that all coefficients have unit root since they satisfy

$$|\hat{\omega}^{c,g}| < 1, \text{ for all } c \text{ and } g \tag{S7}$$

and thus the ARIMA(0,1,0) processes are stationary. This is required for consistent forecasting as otherwise the time series forecast could explode over time. Since the stationarity condition is satisfied, we continue with forecasting of future net mortality rates. Consideration of a different time series model such as described in Enchev et al. (2017) is not needed.

### S.4 Crude mortality forecast: detail

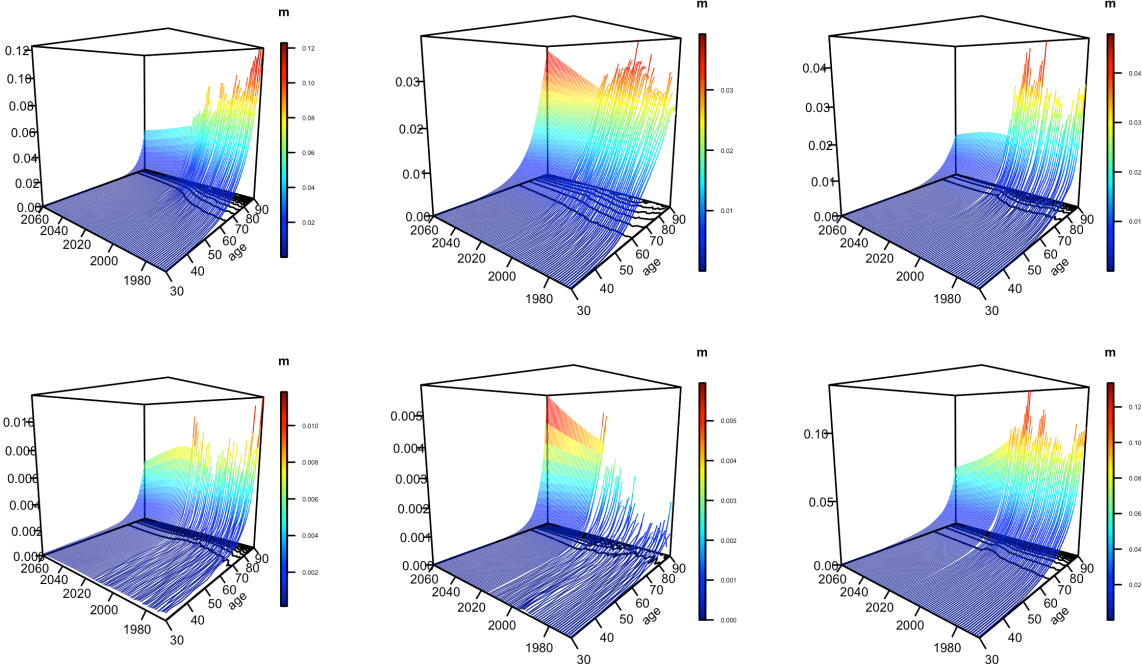


Figure S12: Crude mortality forecast for the Netherlands based on our cause-specific mortality model ( $\theta = 2$ ), male (Frank).

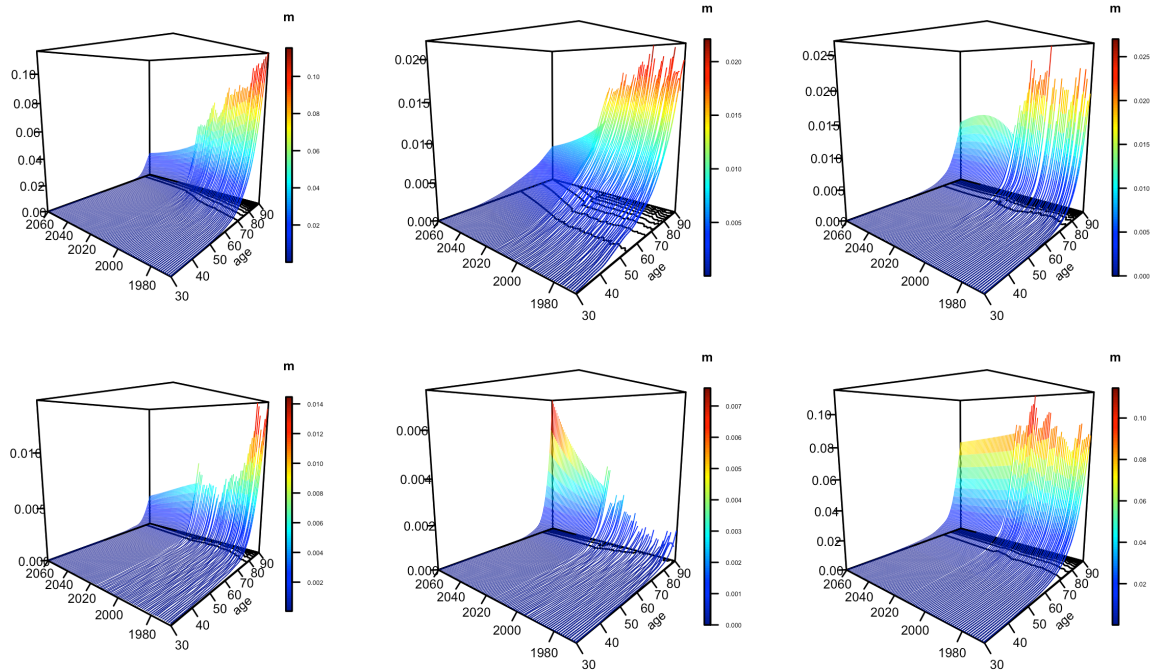


Figure S13: Crude mortality forecast for the Netherlands based on our cause-specific mortality model ( $\theta = 2$ ), female (Frank).

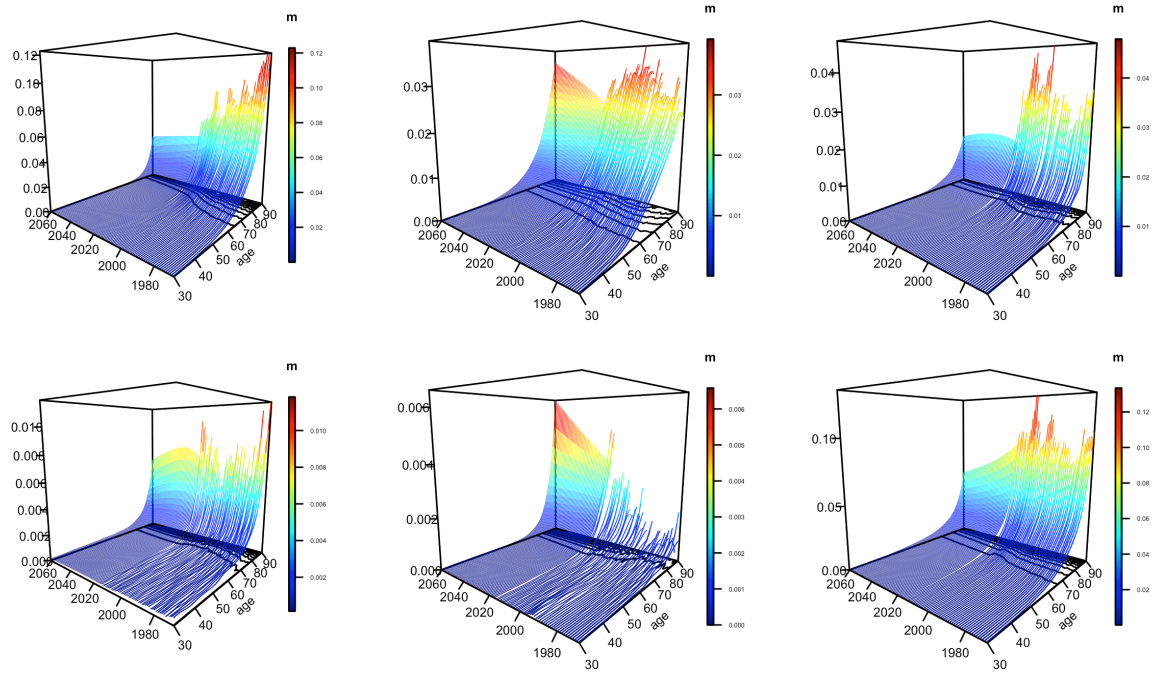


Figure S14: Crude mortality forecast for the Netherlands based on our cause-specific mortality model ( $\theta = 2$ ), male (Clayton).

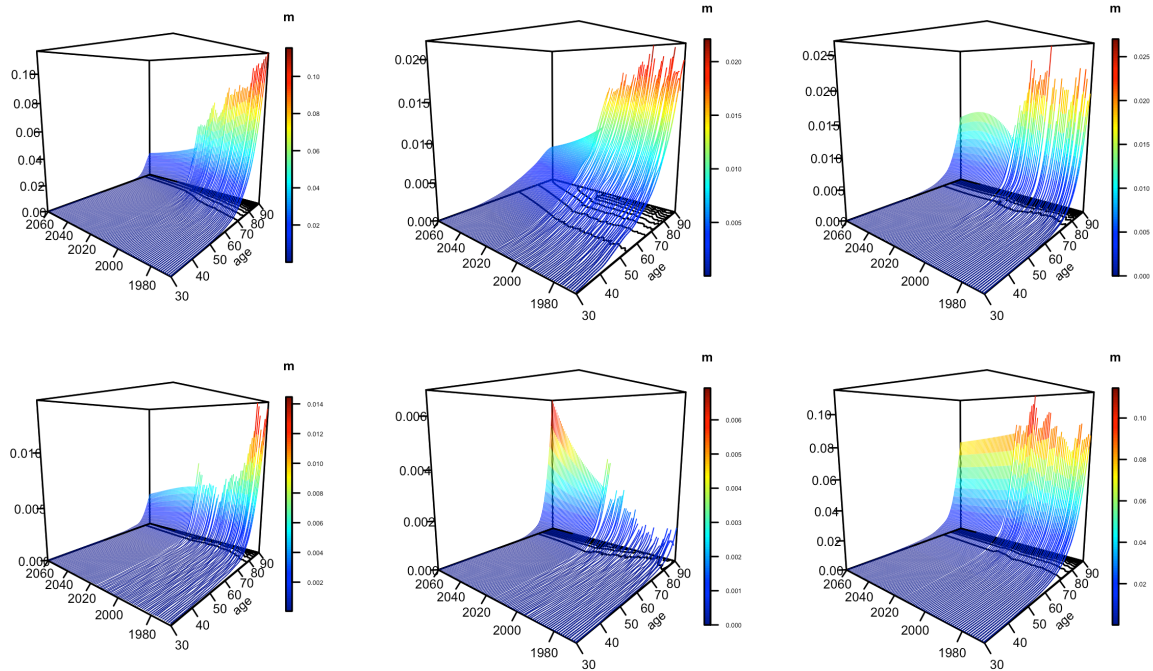


Figure S15: Crude mortality forecast for the Netherlands based on our cause-specific mortality model ( $\theta = 2$ ), female (Clayton).